Further Results on the Range Gating Technique: Visibility in Sea Water

In a preceding paper [1] an analysis of the observation systems employing the range gating technique to enhance visibility through fog was presented. Range gating systems basically consist of an illuminating source emitting short light flashes (e.g., a Q-switched laser) and a gated observation device (e.g., an image converter tube). The time selection of the light collected by the gated observation device allows rejection of backscattered light and full acceptance of useful light coming from the observed objects. Propagation of light at distances of practical interest has to be treated as a multiple scattering process, since the visibility range corresponds to a few attenuation lengths. The multiple scattering problem, including time dependence, has been treated by the Monte Carlo method. The photon path in space is determined by a stochastic selection of the successive scattering events, according to the differential cross section for the elementary scattering process. Brightness and contrast of a standard target, either illuminated or self-luminous, can then be evaluated for various ranges. A comparison with the visibility curves for the eye, allows an estimate of the increase in visibility range to be made.

Some differences in the features of propagation occur between that through sea water and that through fog. These differences are essentially due to the presence in the water of a strong absorption component that is negligible in fog and to the difference in shape of the scattering function in the two instances.

Taking into account these properties, numerical calculations based on the Monte Carlo method have been repeated for sea water, for a wavelength $\lambda = 0.48\ \mu$m corresponding to the well known region of minimum absorption.

As pointed out by Duntley [2], the scattering functions measured in different conditions (measuring set-up and light wavelength) by several authors in various parts of the world,

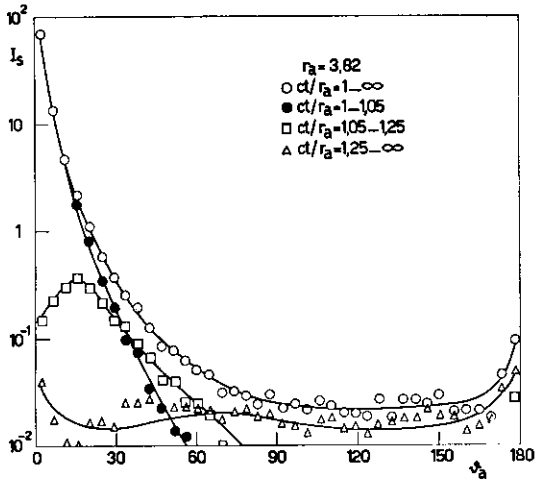

(a)

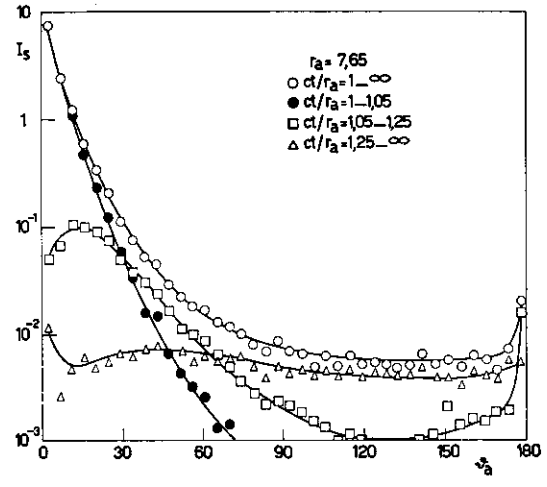

(b)

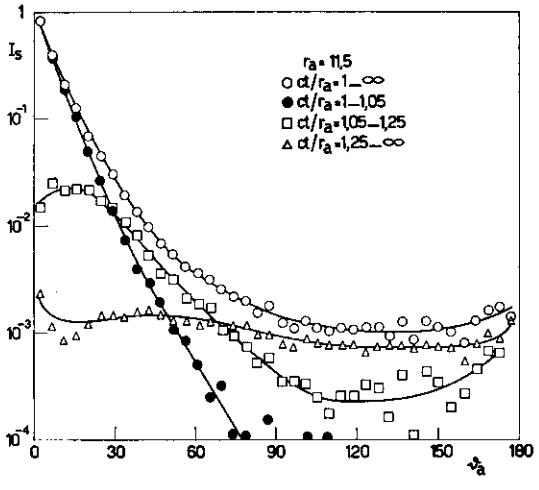

(c)

Figure 1 (a) Light intensity I_S per unit area of collecting surface due to the elementary source versus the angular co-ordinate ϑ_a of the receiving surface, which is placed on a spherical surface of radius $r_a = 3.82$ attenuation length; I_S is plotted for some intervals of the standardized time ct/r_a to evidence the time behaviour. (b) The same as in (a), but for $r_a = 7.65$. (c) The same as in (a), but for $r_a = 11.5$.

yield very similar results especially in the forward scattering region (see fig. 12, reference 2); in the backscattering region the experimental data differ, at most, by a factor of two. From fig. 12 of reference 2 values of the scattering function were averaged between 0° and 165° and the resulting diagram extrapolated linearly between 165° and 180° to give the scattering function that is used in the present calculation. The relative weight of scattering and absorption has been assumed to be 60% and 40% respectively, as given by Duntley (page 218 of reference 2).

Following the model of a spherical scattering volume and of a collecting spherical surface [1], the response of an elementary source with a δ distribution both in space and time has been calculated by the Monte Carlo method.

The results for three different values of the sphere radius r_a, namely $r_a = 3.82$, 7.65 and 11.5 units of attenuation length, are plotted in figs. 1a, b, c. Note that these diagrams, which can be compared to those of figs. 2a, 3a and 4a of reference 1 for fog (since the values assumed for the *scattering* lengths are the same in the two cases) are smoother due to the shape of the scattering function and have a lower amplitude due to the presence of absorption.

From the δ-response, with procedures identical to those introduced in § 3, 4, 5 of reference 1, the behaviour of the contrast C as a function of the angular resolution $\Delta\alpha$ has been obtained. The

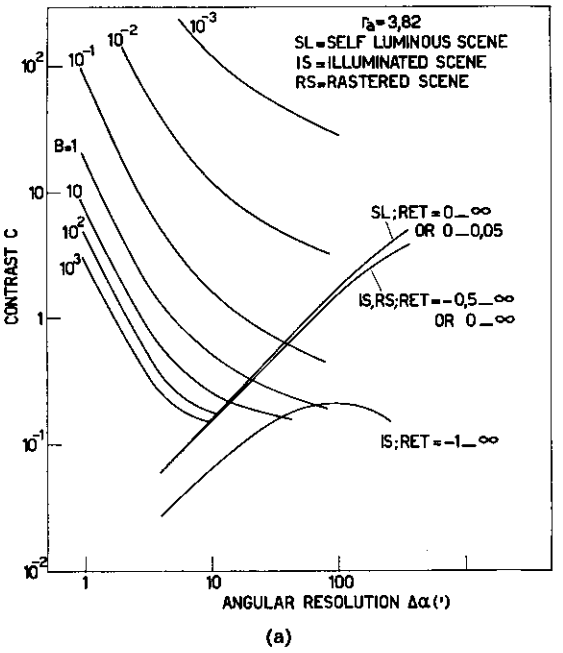

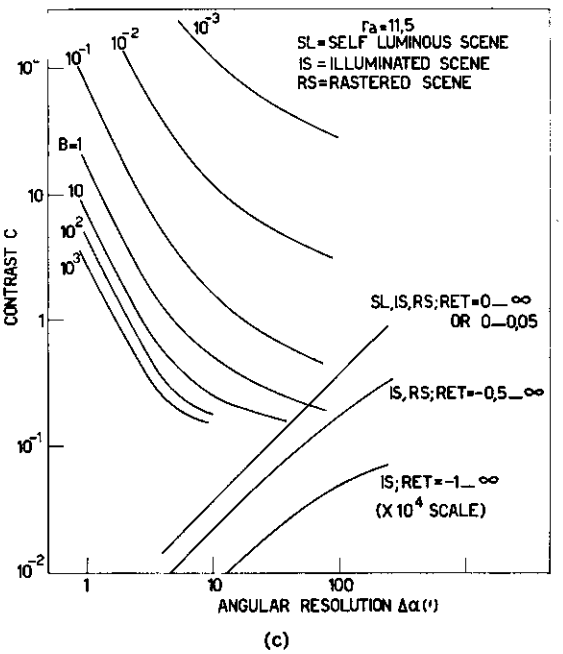

Figure 2 (a) The contrast C against angular resolution $\Delta\alpha$ for different cases of observation at a distance of $r_a = 3.82$ attenuation lengths, showing also the data of Blackwell on the eye sensitivity for various values of background luminance B in foot—Lambert. (b) The same as in (a), but for $r_a = 7.65$. (c) The same as in (a), but for $r_a = 11.5$.

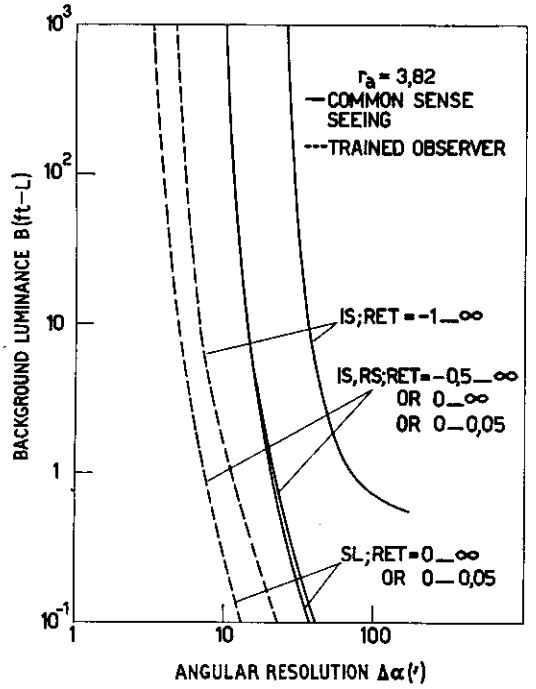

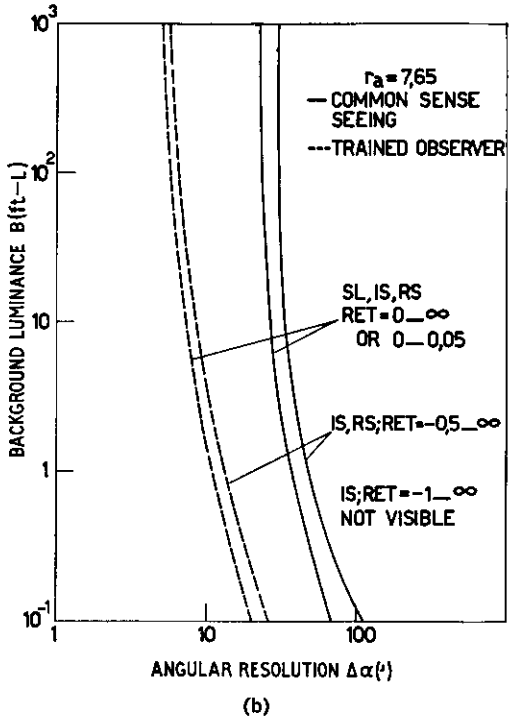

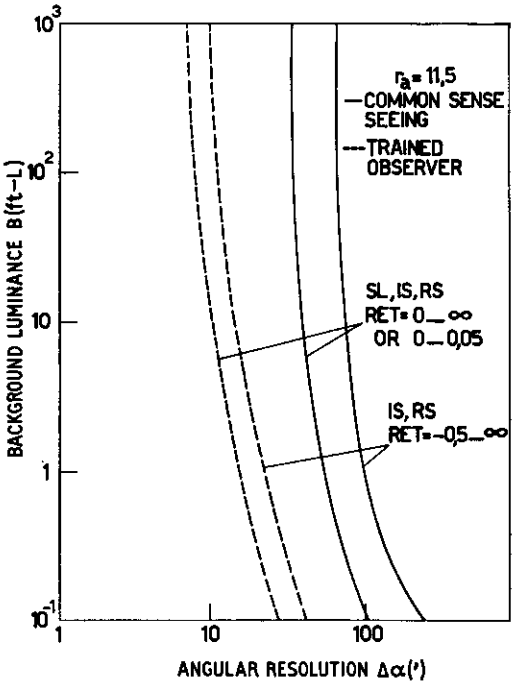

Figure 3 (a) Background luminance B necessary to achieve an angular resolution $\Delta\alpha$ for different cases of observation at a distance $r_a = 3.82$ attenuation lengths. (b) The same as in (a), but for $r_a = 7.65$. (c) The same as in (a), but for $r_a = 11.5$.

results are plotted in figs. 2a, b, c for three values of range r_a, together with the visibility curves of Blackwell (as discussed in reference 1) connecting background luminance B to contrast C and angular resolution $\triangle\alpha$.

The values of B and $\triangle\alpha$ at the intersections of these curves are plotted in figs. 3a, b, and c, for different kinds of operation including range gating and raster techniques. The diagrams indicate that the naked eye-observed illuminated scene (IS, RET $= -1 \_\_ \infty$) is still visible, though with rough angular resolution, for a range of $r_a = 3.82$ attenuation lengths and then becomes invisible, whereas the range-gated or rastered scene (RS) are still visible at $r_a = 11.5$ attenuation lengths, but however, are never better than the corresponding self luminous (SL) scene. To allow meaningful comparisons, considerations on the useful peak and background light level must be made. The diagrams of figs. 4 and 5 show the behaviour of the useful peak radiance and of the background radiance, respectively, versus the range in attenuation lengths.

We notice that the first part of computer results describes the main features of the propagation process and has general validity (figs. 1a, b, c), whereas the second part refers to the evaluation of the brightness, contrast and

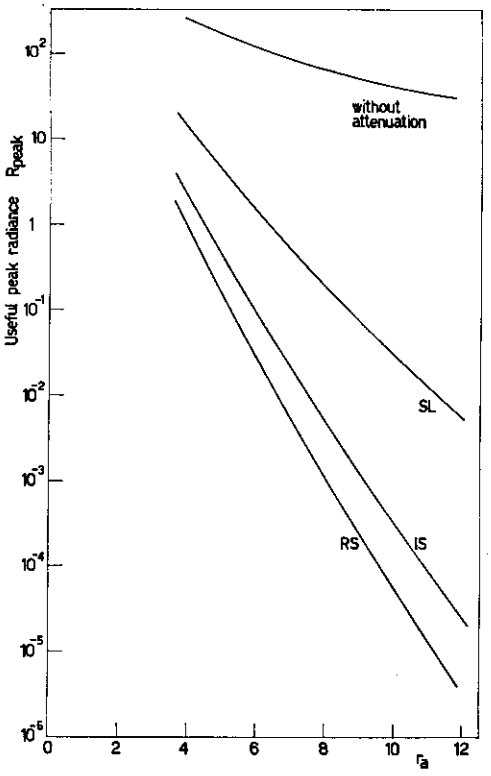

Figure 4 The peak amplitude of radiance R_{peak} as a function of the observation distance r_a in attenuation lengths.

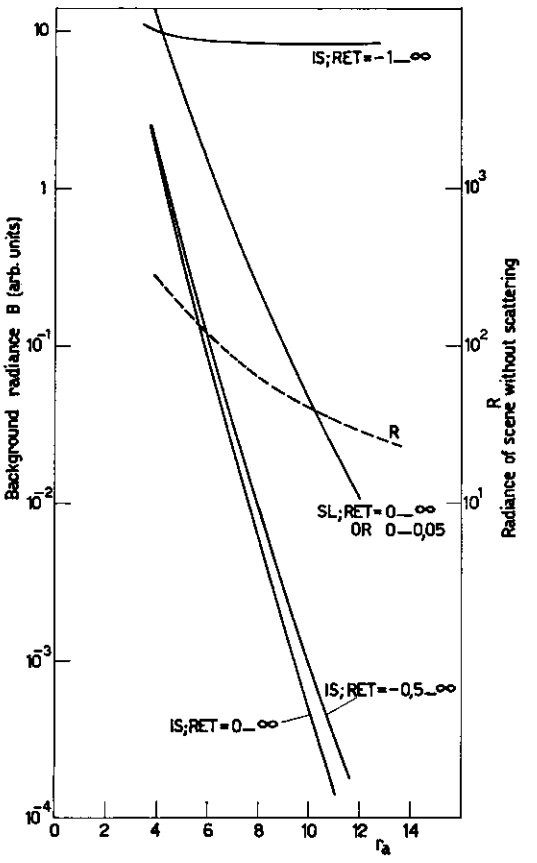

Figure 5 The total background radiance B as a function of the observation distance r_a in attenuation lengths.

visibility of a standard target (a set of concentric black and white rings as shown in fig. 5 of reference 1). With the same procedures, the visibility of different targets and the performances of other arrangements of observation systems could be estimated. As in the case of fog, a visibility enhancement by a factor of between 2 and 3 can be expected from range gating systems with a linear response (e.g. an image converter). If a threshold can be inserted in the image channel (e.g. in the TV signal of the raster system) an additional improvement is expected. In sea water, experiments with a gated image converter operating in connection with a pulsed laser at 5300 Å, were performed by Heckman and Hodgson [3]; their results proved that a visibility range improvement of at least a factor of 2 is obtainable in practice.

Acknowledgement

This work was performed under contract CNR-CISE no. 17.8.3.1 for the Development of Technology and Electronic Instrumentation.

References

1. S. DONATI and A. SONA, *Opto-electronics* **1** (1969 89-101.
2. S. Q. DUNTLEY, *J. Opt. Soc. Amer.* **53** (1963) 214-233.
3. P. HECKMAN JR. and R. T. HODGSON, *IEEE J. Quantum Electronics* **QE-3** (1967) 445-448.

List of Principal Symbols and Notations

R – Light radiance at the observation point
R_{peak} – Peak amplitude of useful light radiance
r_a – radius of the sphere in which propagation takes place; also, distance of schematic scene from the observer
RET – $= ct/r_a - 1$, i.e. relative excess time spent by scattered light (with respect to unscattered) to reach the observer.
t – time elapsed from the instant of light pulse emission by the source
ϑ_a – angular co-ordinate of a point on the spherical collecting surface; it is evaluated with respect to the direction of the elementary δ-source

IS – illuminated scene case: the scene is illuminated by a source placed near the observer

RS – rastered scene case: a TV-like scanning of the scene by a narrow light beam is performed, and combined with a gating of the detector

SL – self-luminous scene case: the scene is either self-luminous or illuminated by a source close to it.

15 August 1969

S. DONATI
A. SONA
Laboratori CISE, Segrate (Milano), Italy